Dual mechanisms of Bcl-2 regulation in IP_3-receptor-mediated Ca^{2+} release: A computational study

Hong Qi(祁宏), Zhi-Qiang Shi(史志强), Zhi-Chao Li(李智超), Chang-Jun Sun(孙长君), Shi-Miao Wang(王世苗), Xiang Li(李翔), and Jian-Wei Shuai(帅建伟)

Citation: Chin. Phys. B, 2021, 30 (**10**): 108704. DOI: 10.1088/1674-1056/ac1e0d
Journal homepage: http://cpb.iphy.ac.cn; http://iopscience.iop.org/cpb

What follows is a list of articles you may be interested in

Effective suppression of beta oscillation in Parkinsonian state via a noisy direct delayed feedback control scheme

Hai-Tao Yu(于海涛), Zi-Han Meng(孟紫寒), Chen Liu(刘晨), Jiang Wang(王江), and Jing Liu(刘静)
Chin. Phys. B, 2021, 30 (**3**): 038703. DOI: 10.1088/1674-1056/abd395

Dynamics and coherence resonance in a thermosensitive neuron driven by photocurrent

Ying Xu(徐莹), Minghua Liu(刘明华), Zhigang Zhu(朱志刚), Jun Ma(马军)
Chin. Phys. B, 2020, 29 (**9**): 098704. DOI: 10.1088/1674-1056/ab9dee

Generating mechanism of pathological beta oscillations in STN-GPe circuit model: A bifurcation study

Jing-Jing Wang(王静静), Yang Yao(姚洋), Zhi-Wei Gao(高志伟), Xiao-Li Li(李小俚), Jun-Song Wang(王俊松)
Chin. Phys. B, 2020, 29 (**5**): 058701. DOI: 10.1088/1674-1056/ab7e9b

Analytically determining frequency and amplitude of spontaneous alpha oscillation in Jansen's neural mass model using the describing function method

Yao Xu(徐瑶), Chun-Hui Zhang(张春会), Ernst Niebur, Jun-Song Wang(王俊松)
Chin. Phys. B, 2018, 27 (**4**): 048701. DOI: 10.1088/1674-1056/27/4/048701

Effects of A1 site occupation on dielectric and ferroelectric properties of $Sr_4CaRTi_3Nb_7O_{30}$ (R=Ce, Eu) tungsten bronze ceramics

Fang Yu-Jiao, Gong Gao-Shang, Gebru Zerihun, Yuan Song-Liu
Chin. Phys. B, 2014, 23 (**12**): 128701. DOI: 10.1088/1674-1056/23/12/128701

Dual mechanisms of Bcl-2 regulation in IP_3-receptor-mediated Ca^{2+} release: A computational study*

Hong Qi(祁宏)[1,2,†], Zhi-Qiang Shi(史志强)[1,3], Zhi-Chao Li(李智超)[1,3], Chang-Jun Sun(孙长君)[1,3], Shi-Miao Wang(王世苗)[3], Xiang Li(李翔)[4,5], and Jian-Wei Shuai(帅建伟)[4,5,‡]

[1] *Complex Systems Research Center, Shanxi University, Taiyuan* 030006, *China*

[2] *Shanxi Key Laboratory of Mathematical Techniques and Big Data Analysis on Disease Control and Prevention, Shanxi University, Taiyuan* 030006, *China*

[3] *School of Mathematical Sciences, Shanxi University, Taiyuan* 030006, *China*

[4] *Department of Physics and Fujian Provincial Key Laboratory for Soft Functional Materials Research, Xiamen University, Xiamen* 361005, *China*

[5] *State Key Laboratory of Cellular Stress Biology, Innovation Center for Cell Signaling Network, and National Institute for Data Science in Health and Medicine, Xiamen University, Xiamen* 361005, *China*

(Received 26 April 2021; revised manuscript received 1 August 2021; accepted manuscript online 17 August 2021)

Inositol 1,4,5-trisphosphate receptors (IP_3R)-mediated calcium ion (Ca^{2+}) release plays a central role in the regulation of cell survival and death. Bcl-2 limits the Ca^{2+} release function of the IP_3R through a direct or indirect mechanism. However, the two mechanisms are overwhelmingly complex and not completely understood. Here, we convert the mechanisms into a set of ordinary differential equations. We firstly simulate the time evolution of Ca^{2+} concentration under two different levels of Bcl-2 for the direct and indirect mechanism models and compare them with experimental results available in the literature. Secondly, we employ one- and two-parameter bifurcation analysis to demonstrate that Bcl-2 can suppress Ca^{2+} signal from a global point of view both in the direct and indirect mechanism models. We then use mathematical analysis to clarify that the indirect mechanism is more efficient than the direct mechanism in repressing Ca^{2+} signal. Lastly, we predict that the two mechanisms restrict Ca^{2+} signal synergistically. Together, our study provides theoretical insights into Bcl-2 regulation in IP_3R-mediated Ca^{2+} release, which may be instrumental for the successful development of therapies to target Bcl-2 for cancer treatment.

Keywords: Ca^{2+}, Bcl-2, bifurcation analysis, oscillations

PACS: 87.16.Vy, 87.17.Aa, 87.18.Vf **DOI:** 10.1088/1674-1056/ac1e0d

1. Introduction

Calcium ion (Ca^{2+}) is a highly versatile signaling molecule in the cell. It can control many important physiological processes and so is necessary for cell survival.[1,2] Under resting conditions, most of the Ca^{2+} in the cell is stored in the endoplasmic reticulum (ER), and cytosolic Ca^{2+} concentration ($[Ca^{2+}]$) is maintained at low levels. The homeostasis of $[Ca^{2+}]$ is dynamically regulated by active Ca^{2+} uptake through sarco/endoplasmic reticulum Ca^{2+}-ATPase (SERCA) and passive Ca^{2+} leak from the ER. Upon stimuli, IP_3 (inositol 1,4,5-trisphosphate) forms and binds to IP_3 receptor (IP_3R) to release Ca^{2+} from the ER, generating the upstroke of a Ca^{2+} oscillation. The SERCA then pumps the released Ca^{2+} back into the ER, completing the Ca^{2+} oscillation.[3] The resulting Ca^{2+} oscillations display different amplitudes and periods, thereby regulating different cellular functions.[3] However, excessive elevations of $[Ca^{2+}]$ always trigger a series of catastrophic events, leading to cytosolic Ca^{2+} overload-driven cell death.[2–4]

Because of the delicate role of Ca^{2+} in both cell survival and death, IP_3R-mediated Ca^{2+} release must be carefully balanced.[5] This release is exquisitely modulated by Ca^{2+} itself,[6] or by an expanding group of messengers, such as IP_3,[7] cytochrome c,[8] and Bcl-2 (B-cell lymphoma-2). In addition to its well-known pro-survival role by counteracting mitochondrial outer membrane permeabilization at the mitochondria,[9] Bcl-2 also prevents cell death by preventing excessive IP_3R-mediated Ca^{2+} elevation at the ER.[10,11] Recent experimental studies revealed that Bcl-2 can suppress IP_3R-mediated Ca^{2+} release from the ER via two distinct mechanisms. On the one hand, Bcl-2 via its BH4 domain directly binds to the regulatory and coupling region of IP_3R, preventing IP_3R-mediated Ca^{2+} release, thereby inhibiting Ca^{2+} induced cell death.[12–15] On the other hand, Bcl-2 serves as a docking platform for both calcineurin (CaN) and dopamine- and cAMP-regulated phosphoprotein of 32 kDa (DARPP-32), createing a negative feedback loop that regulates IP_3R phosphorylation and thus indirectly prevents Ca^{2+} elevation that induces cell death.[16] We term the first one "direct mechanism", and the second one "indirect mechanism".

*Project supported by Shanxi Province Science Foundation for Youths (Grant No. 201901D211159) and the National Natural Science Foundation of China (Grant Nos. 11504214, 11874310, and 12090052).

†Corresponding author. E-mail: hongqi@sxu.edu.cn

‡Corresponding author. E-mail: jianweishuai@xmu.edu.cn

Despite these experimental results, the global dynamic behaviors of Bcl-2 inhibition in IP_3R-mediated Ca^{2+} signaling are not completely understood due to the complex interactions among the components that involved in the direct or indirect mechanism. In particular, it remains unexplored how they jointly affect Ca^{2+} signal and which mechanism is more potent in the suppression of Ca^{2+} release.

Although the dynamic mechanisms underlying cellular signaling seem overwhelmingly complex, they can be clearly understood by the mathematical modeling using ordinary differential equations (ODEs) based on biochemical kinetics.[3,17–20] Recently, we have constructed a model to systematically study the signaling pathway of Ca^{2+} release regulated by Bcl-2 indirectly,[21] which can be called the indirect mechanism model. In the current study, we develop a direct mechanism model and integrate it into the indirect mechanism model. We employ these two mechanism models, separately and in combination, to further dissect the inhibitory effect of Bcl-2 on Ca^{2+} signal theoretically. In particular, we demonstrate that the indirect mechanism is more potent than the direct mechanism in preventing Ca^{2+} release from the ER and that the two mechanisms dampen Ca^{2+} signal synergistically. Since Bcl-2 suppression in Ca^{2+} release is exploited by cancer cells to escape cell death, the present study may shed light on future therapeutic approaches for the treatment of cancer.

2. Model

As the model is complex, we shall describe it in the following steps:

(1) A general Ca^{2+} oscillation model.

(2) The details of the direct mechanism model (Fig. 1(a)).

(3) The details of the indirect mechanism model (Fig. 1(b)).

(4) How the two models are incorporated together into a dualmechanism model (Fig. 1(c)).

(5) How to determine the model parameters.

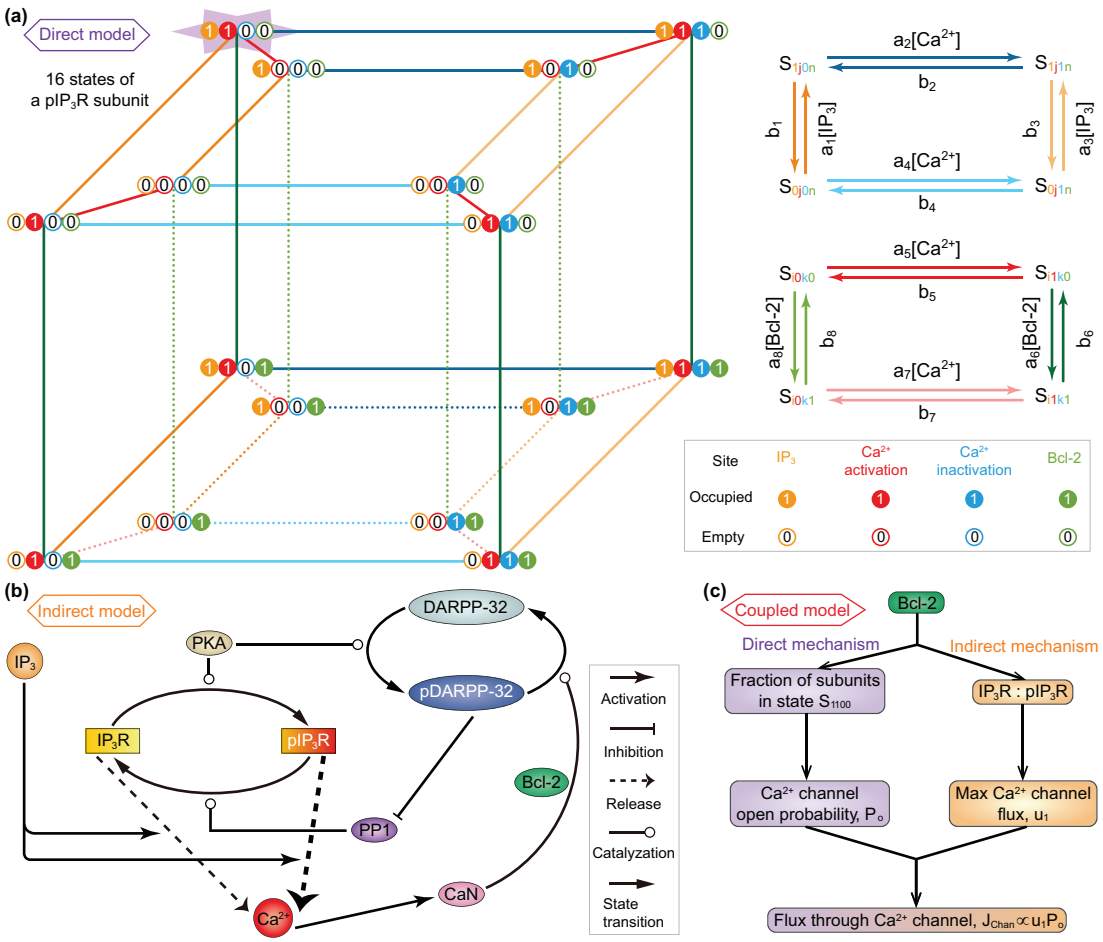

Fig. 1. (a) Kinetic schemes of the direct mechanism model. For simplify, it is assumed that all IP_3Rs are phosphorylated (pIP_3R). Left: Each subunit of pIP_3R has one IP_3 binding site, two Ca^{2+} binding sites, and one Bcl-2 binding site. These sites can be occupied (represented by 1) or empty (represented by 0), and thus there are sixteen possible states (see from the top view). Right: The kinetics on the top and bottom faces of the inner and outer cubes as well as the kinetics between the two cubes. (b) Schematic diagram of the indirect mechanism model. The reversible conversion between phosphorylated and non-phosphorylated forms of IP_3R is catalyzed by PKA and PP1. IP_3 binds to IP_3R/pIP_3R and modulates Ca^{2+} release. The release of Ca^{2+} from pIP_3R is stronger than that from IP_3R. An increase in Ca^{2+} level leads to activation of CaN, which dephosphorylates pDARPP-32 into DARPP-32. During this process, Bcl-2 serves as a platform docking CaN and pDARPP-32. PKA catalyzes DARPP-32 into pDARPP-32, which is an inhibitor of PP1. (c) Mechanism of the coupled model. The direct and indirect mechanisms are linked by Bcl-2 regulation of flux through Ca^{2+} channel, i.e., IP_3R and pIP_3R. The direct mechanism influences the channel open probability by determining the fraction of channel subunits in state S_{1100}, while the indirect mechanism influences the maximal channel flux by determining the IP_3R-to-pIP_3R ratio.

2.1. Ca^{2+} oscillation model

For a closed cell, Ca^{2+} oscillations mainly derive from three types of fluxes between the ER and the cytosol: IP_3R channel-mediated Ca^{2+} release from the ER into the cytosol (J_{Chan}), Ca^{2+} leakage from the ER into the cytosol (J_{Leak}), and SERCA-dependent Ca^{2+} uptake from the cytosol into the ER (J_{SERCA}).

The driving force for Ca^{2+} flow from the ER to the cytoplasm is the concentration difference between them. We get

$$J_{Chan} = u_1 P_o \left([Ca^{2+}]_{ER} - [Ca^{2+}] \right), \tag{1}$$

$$J_{Leak} = u_2 \left([Ca^{2+}]_{ER} - [Ca^{2+}] \right). \tag{2}$$

Here, P_o is the open probability of the IP_3R channel, u_1 is the maximal Ca^{2+} channel flux, and u_2 is the Ca^{2+} leak flux constant. ER Ca^{2+} concentration ($[Ca^{2+}]_{ER}$) is determined by conservation condition $c_0 = c_1[Ca^{2+}]_{ER} + [Ca^{2+}]$.

The SERCA-dependent Ca^{2+} pump is described by a Hill equation, with a Hill coefficient of 2,

$$J_{SERCA} = \frac{u_3 [Ca^{2+}]^2}{K_{SERCA}^2 + [Ca^{2+}]^2}, \tag{3}$$

where u_3 is the maximal uptake flux of Ca^{2+}, and K_{SERCA} is the activation constant for SERCA.

2.2. Direct mechanism model

In construction, the direct mechanism model is based on De Young–Keizer model. De Young and Keizer assumed that three equivalent and independent subunits are involved in the opening of an IP_3R, each subunit of which has one IP_3 binding site, one activating Ca^{2+} binding site, and one inhibiting Ca^{2+} binding site.[22] According to the experimental results,[12–15] Bcl-2 directly binds to the IP_3R, so we can assume that each subunit has one Bcl-2 binding site. Thus, each subunit of IP_3R may exist in sixteen states with transitions governed by binding rates (a_i) and unbinding rates (b_i). The state of each subunit is denoted as S_{ijkn}, where the index i represents the IP_3 binding site, j the activating Ca^{2+} binding site, k the inhibiting Ca^{2+} binding site, and n the Bcl-2 binding site. An occupied site is represented by 1, and an empty site by 0. The fraction of subunits in state S_{ijkn} is denoted by x_{ijkn}.

According to the law of mass action, the ODEs describing the dynamics of a subunit can be written down. Due to the space limitation, only the ODE for x_{1100} is presented in the main text,

$$\begin{aligned} \frac{dx_{1100}}{dt} &= a_1[IP_3]x_{0100} + b_2 x_{1110} + a_5[Ca^{2+}]x_{1000} + b_6 x_{1101} \\ &\quad - \left(b_1 + a_2[Ca^{2+}] + b_5 + a_6[\text{Bcl-2}]\right) x_{1100}, \end{aligned} \tag{4}$$

and the other fifteen ODEs are given in the supplementary material.

Similar to the consideration of De Young–Keizer model,[22] we further assume that a subunit is active only when IP_3 and activating Ca^{2+} sites are occupied but inhibiting Ca^{2+} and Bcl-2 sites are unoccupied (S_{1100}) and that all three subunits must be in this state for the IP_3R channel to be open. With these assumptions, P_o is written as

$$P_o = x_{1100}^3. \tag{5}$$

2.3. Indirect mechanism model

The IP_3R (herein refers to type-1 IP_3R, whose amino acid at position 1755 is serine) has two forms: phosphorylated (pIP_3R) and non-phosphorylated (IP_3R), and phosphorylation results in enhanced Ca^{2+} release.[23] If we let k denote the maximal Ca^{2+} release rate per micromole of IP_3R, and let α denote the release rate ratio of pIP_3R to IP_3R ($1 < \alpha \leq 9$), u_1 mentioned above can be modified as

$$u_1 = \frac{k}{1+\alpha}[IP_3R] + \frac{\alpha k}{1+\alpha}[pIP_3R]. \tag{6}$$

As done in our previous work, we set $\alpha = 6$, because we have demonstrated that the value of α will not significantly affect our result.[21]

The transition between the two forms of IP_3R is catalyzed by two enzymes: protein kinase A (PKA) which phosphorylates IP_3R at Ser1755 into pIP_3R and protein phosphatase 1 (PP1) which dephosphorylates pIP_3R into IP_3R.[24] Phosphorylation and dephosphorylation rates are often modeled by Michaelis–Menten equation,[25] thus,

$$v_1 = \frac{v_{PKA1}[PKA][IP_3R]}{K_{IP_3R} + [IP_3R]}, \tag{7}$$

$$v_2 = \frac{v_{PP1}[PP1][pIP_3R]}{K_{pIP_3R} + [pIP_3R]}, \tag{8}$$

where v_{PKA1} and v_{PP1} are the maximal reaction rate, and K_{IP3R} and K_{pIP3R} are the Michaelis constants.

CaN is a Ca^{2+}-activated protein phosphatase that has four Ca^{2+} binding sites. Ca^{2+} binding sites 1 and 2 are of lower affinity with K_ds (dissociation constants) in the micromolar range, whereas Ca^{2+} binding sites 3 and 4 are of higher affinity with K_ds in the nanomolar range.[26] So we only consider the first two binding sites, and the evolution for active CaN (CaN^*) is assumed to be given by mass-action kinetics

$$\frac{d[CaN^*]}{dt} = k_1[CaN][Ca^{2+}]^2 - k_2[CaN^*]. \tag{9}$$

In addition, the principle of mass conservation yields

$$[CaN]_{tot} = [CaN] + [CaN^*]. \tag{10}$$

Because the binding and unbinding rates are much faster than the changes of $[CaN^*]$, we use the quasi-steady-state approximation for it and obtain

$$[CaN^*] = \frac{k_1[CaN]_{tot}[Ca^{2+}]^2}{k_1[Ca^{2+}]^2 + k_2}. \tag{11}$$

Bcl-2 serves as a platform, in which CaN* dephosphorylates the phosphorylated DARPP-32 (pDARPP-32) into DARPP-32.[16] The corresponding reaction rate is

$$v_3 = \frac{v_{\mathrm{CaN}^*}[\mathrm{CaN}^*][\mathrm{pDARPP\text{-}32}]}{K_{\mathrm{pD32}} + [\mathrm{pDARPP\text{-}32}]}. \tag{12}$$

Here v_{CaN^*} is the maximal reaction rate of this process, we correlate it with Bcl-2 regulation by a Hill function

$$v_{\mathrm{CaN}^*} = \frac{v_{\mathrm{Bcl-2}}[\mathrm{Bcl\text{-}2}]^4}{K_{\mathrm{Bcl-2}}^4 + [\mathrm{Bcl\text{-}2}]^4}. \tag{13}$$

PKA can also phosphorylate DARPP-32, and the corresponding reaction rate is

$$v_4 = \frac{v_{\mathrm{PKA2}}[\mathrm{PKA}][\mathrm{DARPP\text{-}32}]}{K_{\mathrm{D32}} + [\mathrm{pDARPP\text{-}32}]}. \tag{14}$$

The pDARPP-32 has an inhibitory effect on PP1,[16,24] which can be reflected in the maximal rate of dephosphorylation of $\mathrm{pIP_3R}$ by PP1, thus we let

$$v_{\mathrm{PP1}} = \frac{v'_{\mathrm{PP1}} K_{\mathrm{PP1}}^2}{K_{\mathrm{PP1}}^2 + [\mathrm{pDARPP\text{-}32}]^2}. \tag{15}$$

2.4. Dual-mechanism model

The nexus between the direct mechanism and the indirect mechanism primarily lies in the Bcl-2 regulation of $\mathrm{IP_3R}$ channel, i.e., the term J_{chan} in Eq. (1). The direct mechanism influences P_{o} by determining x_{1100}, while the indirect mechanism influences u_1 by determining the ratio between $\mathrm{IP_3R}$ and $\mathrm{pIP_3R}$. In addition, we assume that for a certain Bcl-2 molecule, it can only participate in either one of the two mechanisms. If we let the proportion of Bcl-2 involved in the direct mechanism be β, then the one involved in the indirect mechanism is $1-\beta$.

The ODEs which describe the dynamical process of all species (except the sixteen states of $\mathrm{IP_3R/pIP_3R}$) involved in the Bcl-2 regulation of $\mathrm{Ca^{2+}}$ signaling are

$$\begin{cases} \dfrac{\mathrm{d}[\mathrm{Ca}^{2+}]}{\mathrm{d}t} = J_{\mathrm{chan}} + J_{\mathrm{leak}} - J_{\mathrm{pump}}, \\ \dfrac{\mathrm{d}[\mathrm{pIP_3R}]}{\mathrm{d}t} = v_1 - v_2, \\ \dfrac{\mathrm{d}[\mathrm{DARPP\text{-}32}]}{\mathrm{d}t} = v_3 - v_4, \end{cases} \tag{16}$$

with two mass conservation equations

$$[\mathrm{IP_3R}]_{\mathrm{tot}} = [\mathrm{IP_3R}] + [\mathrm{pIP_3R}], \tag{17}$$

$$[\mathrm{DARPP\text{-}32}]_{\mathrm{tot}} = [\mathrm{DARPP\text{-}32}] + [\mathrm{pDARPP\text{-}32}]. \tag{18}$$

2.5. Model parameters

The specific meaning of each parameter in the De Young–Keizer model can be found in Ref. [22]. Under its default parameters, the peak value of $\mathrm{Ca^{2+}}$ oscillations is 0.16–0.47 μM, and the period is 11.4–15.6 s. Due to the need to fit the peak value and period of the $\mathrm{Ca^{2+}}$ oscillations in the experiments,[12,16] the values of some relevant parameters in the original model must be rescaled. The parameters in the De Young–Keizer model, together with the binding and unbinding rates of Bcl-2 and $\mathrm{IP_3R}$, constitute the parameters of the direct model (see Table S1). Table S2 lists the parameters of the indirect model, among which the protein concentrations are drawn from Refs. [27–30], reaction rates k_1 and k_2 are obtained from Ref. [29], and the remaining reaction rates are adjusted by fitting the experimental results in Ref. [16]. $[\mathrm{IP_3}]$ and [Bcl-2] are the two independent input variables, and $[\mathrm{Ca^{2+}}]$ is the output variable.

3. Results

Although both the direct mechanism and indirect mechanism of the Bcl-2 regulation of $\mathrm{Ca^{2+}}$ signaling can be present simultaneously, it is better to first capture their respective roles. After separately evaluating the respective roles of the direct mechanism and indirect mechanism, we then examine the comprehensive effects of the dual mechanisms.

3.1. Time course of $\mathrm{Ca^{2+}}$ signaling

As for the direct mechanism model, all $\mathrm{IP_3Rs}$ are postulated to be in the phosphorylated form. We do not consider the dephosphorylated form based on the following two considerations. On the one hand, to our best knowledge, there is no reference available for measuring the ratio of phosphorylated to dephosphorylated $\mathrm{IP_3R}$. Nonetheless, it is clearly that the $\mathrm{pIP_3R}$ is the dominant form for releasing $\mathrm{Ca^{2+}}$.[23] On the other hand, the concurrent consideration of the two forms will make each $\mathrm{IP_3R}$ subunit have a phosphorylation binding site, and there will be five binding sites in total, which will make the modelling very complex. Moreover, the results obtained by the opposite postulate (Fig. S1) reveal that it only has a limited impact on the conclusion. The time-course plots show that when [Bcl-2] = 0.15 μM the peak value of $\mathrm{Ca^{2+}}$ oscillations is more than 0.28 μM (Fig. 2(a)), while when [Bcl-2] = 0.3 μM the peak value is about 0.17 μM (Fig. 2(b)).

As for the indirect mechanism model, an $\mathrm{IP_3R}$ exists in either phosphorylated or unphosphorylated form, the transition of which is regulated by PKA and PP1. The time-course plots show that when [Bcl-2] = 0.15 μM the peak value of $\mathrm{Ca^{2+}}$ oscillations is more than 0.34 μM (Fig. 2(c)), while when [Bcl-2] = 0.3 μM the peak value is about 0.12 μM (Fig. 2(d)).

Although the results of Fig. 2 indicate that Bcl-2 seems to have an effect on the frequency of $\mathrm{Ca^{2+}}$ oscillations, the two core references[12,16] underlying our modeling work do not mention the impact of Bcl-2 on the frequency. Furthermore, we have recently demonstrated that it is the amplitude, but not the frequency of $\mathrm{Ca^{2+}}$ oscillations that regulates apop-

tosis induction.[3] Hence, we hereafter only focus on the effect of Bcl-2 on the amplitude of Ca^{2+} oscillations.

Taken together, both the direct mechanism model and the indirect mechanism model indicate that Bcl-2 has an inhibitory effect on Ca^{2+} oscillations, and the simulation results are qualitatively consistent with the observations.[12,16]

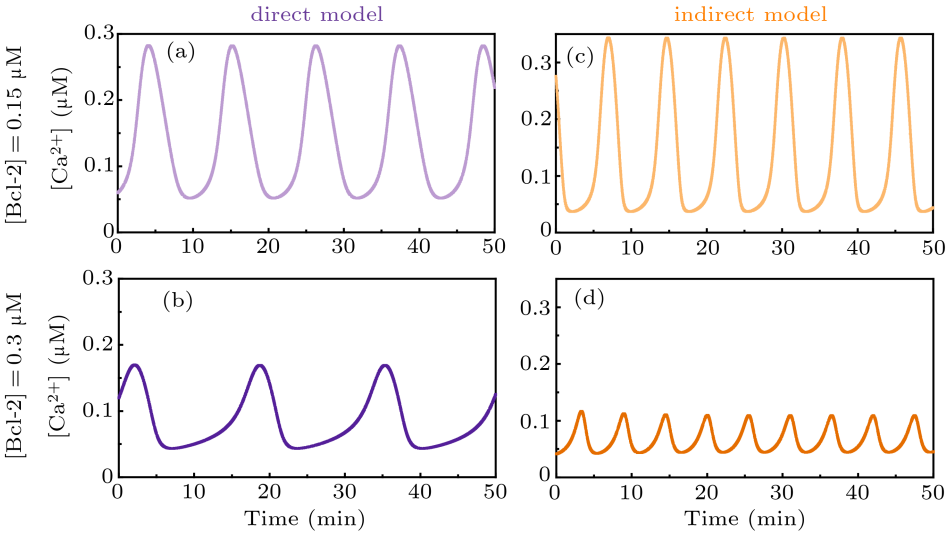

Fig. 2. Time course of Ca^{2+} signal for direct mechanism model when [Bcl-2] is 0.15 μM (a) and 0.3 μM (b), respectively. Time course of Ca^{2+} signal for indirect mechanism model when [Bcl-2] is 0.15 μM (c) and 0.3 μM (d), respectively.

3.2. One-parameter bifurcation analysis

Next we use one-parameter bifurcation diagram to character the influence of Bcl-2 on Ca^{2+} signal from a global point of view. The Hopf bifurcation diagrams in Fig. 3 illustrate that when [Bcl-2] is used as a control parameter, a stable steady state loses stability and gives birth to limit-cycle oscillations, which are born at the Hopf bifurcation point (abbreviated as BP).

The similarities between the direct mechanism model and the indirect mechanism model are: (1) for [Bcl-2] $<$ BP1, there is one stable steady state corresponding to higher [Ca^{2+}]; (2) for [Bcl-2] $>$ BP2, there is one stable steady state corresponding to lower [Ca^{2+}]; (3) for BP1 $<$ [Bcl-2] $<$ BP2, the amplitude of Ca^{2+} oscillations first increases and then decreases when [Bcl-2] increases, but in a broad parameter range it decreases with increasing [Bcl-2]. The major distinction between them is that the BP1 of the direct mechanism model is a supercritical Hopf bifurcation point (Fig. 3(a)), while the BP1 of the indirect mechanism model is a subcritical Hopf bifurcation point (Fig. 3(b)). The difference between the supercritical and subcritical Hopf bifurcation points is that a stable limit cycle with small amplitude appears at the former, whereas at the latter an unstable limit cycle occurs, the amplitude of which grows quickly until it connects with the large amplitude, stable limit cycle.[31]

Collectively, the one-parameter bifurcation analysis for the direct mechanism model and the indirect mechanism model suggests that Bcl-2 can inhibit Ca^{2+} release from the ER.

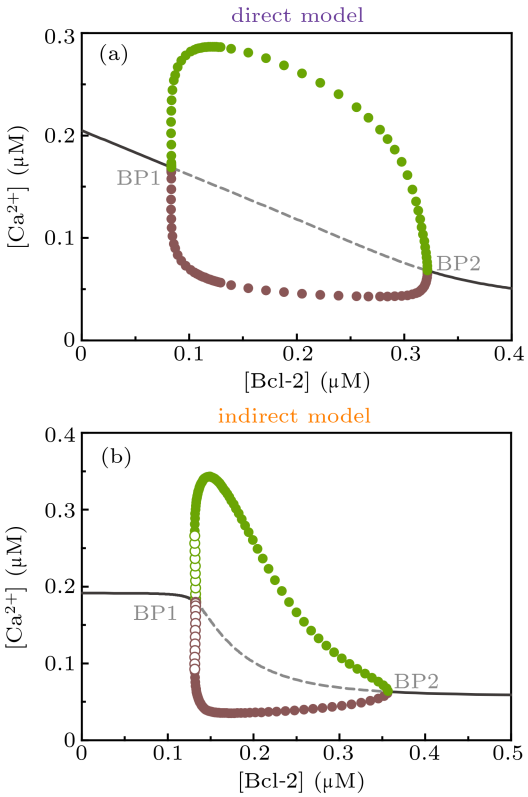

Fig. 3. One-parameter bifurcation diagrams of [Ca^{2+}] against [Bcl-2] for direct mechanism model (a) and indirect mechanism model (b). Solid/dashed line: stable/unstable steady state; filled/empty circle: maximal (green) and minimal (brown) values attained by a stable/unstable limit cycle oscillation. BP, bifurcation point.

3.3. Two-parameter bifurcation analysis

The above results are obtained under the condition of a fixed [IP_3]. We next employ two-parameter bifurcation analysis to further assess the effects of simultaneous inputs, i.e., a

varied combination of [IP_3] and [Bcl-2], on Ca^{2+} oscillations.

In the two-parameter bifurcation diagrams (Fig. 4), stable limit-cycle oscillations only occur within the color regions, which correspond to the appropriate parameter combinations of [IP_3] and [Bcl-2]. Here, we focus on the peak value of Ca^{2+} oscillations because excessive Ca^{2+} elevation triggers cell death.[3,16] Figure 4(a) displays that for the direct mechanism model, although Bcl-2 may elevate the peak value in a narrow parameter interval at the left border, it represses the peak value in a broad parameter space. For the indirect mechanism model (Fig. 4(b)), the peak value of Ca^{2+} oscillations caused by a fixed [IP_3] for a higher [Bcl-2] is always significantly smaller than the one for a lower [Bcl-2], suggesting that Bcl-2 suppresses the peak value.

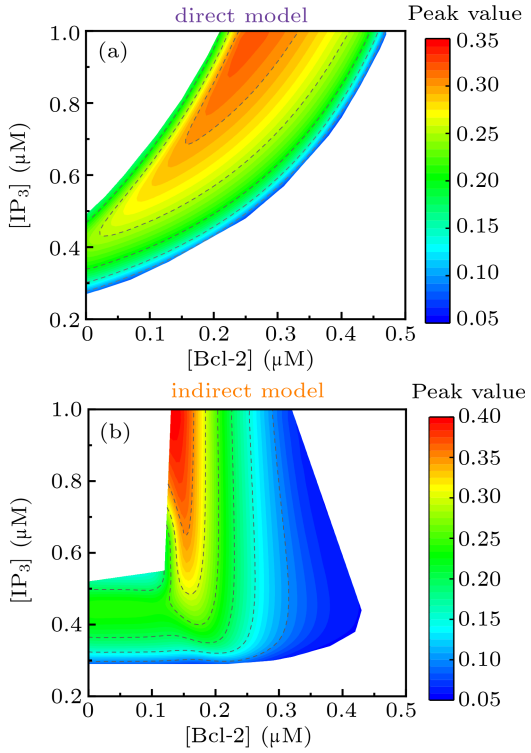

Fig. 4. Two-parameter bifurcation diagrams of the peak of [Ca^{2+}] as a function of [Bcl-2] and [IP_3] for direct mechanism model (a) and indirect mechanism model (b). Ca^{2+} oscillations only occur within the color region.

In both the direct mechanism model and the indirect mechanism model, as [Bcl-2] increases, it first passes a Hopf bifurcation point (e.g., BP1 in Fig. 3), where Ca^{2+} oscillations appear with small amplitude and grow larger as [Bcl-2] is increased further. In the indirect mechanism model, the bifurcation point is a supercritical Hopf bifurcation point, where stable Ca^{2+} oscillations with large amplitude appear abruptly. These are the mathematical foundations underlying the appearance at the left boundary of the oscillation region.

In summary, the two-parameter bifurcation analysis for the direct mechanism model and the indirect mechanism model demonstrates that Bcl-2 can restrain exaggerated Ca^{2+} release.

3.4. Mathematical analysis

All the above findings indicate that the indirect mechanism seems to be more effective in suppressing Ca^{2+} signal than the direct mechanism. Specifically, the indirect mechanism not only suppresses the oscillation amplitude (especially the peak value) in a larger range, but also suppresses the peak value more potently. In the following, we use mathematical analysis to quantify their efficiency in repressing Ca^{2+} flux from Ca^{2+} channel, i.e., IP_3R and pIP_3R.

In the direct mechanism, the Ca^{2+} channel is occupied by Bcl-2, which pulls it away from the open state. The channel open probability can be calculated by the deterministic matrix transition method.[32,33] When the system is in equilibrium, x_{ijkn} can be expressed by x_{0000}, for example,

$$x_{1000} = \frac{[IP_3]}{d_1} x_{0000},$$
$$x_{1100} = \frac{[Ca^{2+}]}{d_5} \frac{[IP_3]}{d_1} x_{0000},$$
$$x_{1101} = \frac{[\text{Bcl-2}]}{d_6} \frac{[Ca^{2+}]}{d_5} \frac{[IP_3]}{d_1} x_{0000}.$$

Then the normalized equilibrium probability for state $(ijkn)$ is

$$X_{ijkn} = \frac{x_{ijkn}}{Z},$$

where $Z = \Sigma x_{ijkn}$, i.e.,

$$\begin{aligned} Z = 1 &+ \frac{[IP_3]}{d_1} + \frac{[Ca^{2+}]}{d_4} + \frac{[Ca^{2+}]}{d_5} + \frac{[\text{Bcl-2}]}{d_8} + \frac{[IP_3]}{d_1}\frac{[Ca^{2+}]}{d_2} \\ &+ \frac{[IP_3]}{d_1}\frac{[Ca^{2+}]}{d_5} + \frac{[Ca^{2+}]}{d_4}\frac{[Ca^{2+}]}{d_5} + \frac{[Ca^{2+}]}{d_5}\frac{[\text{Bcl-2}]}{d_6} \\ &+ \frac{[IP_3]}{d_1}\frac{[\text{Bcl-2}]}{d_8} + \frac{[Ca^{2+}]}{d_4}\frac{[\text{Bcl-2}]}{d_8} + \frac{[IP_3]}{d_1}\frac{[Ca^{2+}]}{d_2}\frac{[Ca^{2+}]}{d_5} \\ &+ \frac{[IP_3]}{d_1}\frac{[Ca^{2+}]}{d_2}\frac{[\text{Bcl-2}]}{d_8} + \frac{[IP_3]}{d_1}\frac{[Ca^{2+}]}{d_5}\frac{[\text{Bcl-2}]}{d_6} \\ &+ \frac{[Ca^{2+}]}{d_4}\frac{[Ca^{2+}]}{d_5}\frac{[\text{Bcl-2}]}{d_6} + \frac{[IP_3]}{d_1}\frac{[Ca^{2+}]}{d_2}\frac{[Ca^{2+}]}{d_5}\frac{[\text{Bcl-2}]}{d_6}. \end{aligned}$$

Therefore, the normalized equilibrium probability for the open state is

$$X_{1100} = \frac{[Ca^{2+}]}{d_5} \frac{[IP_3]}{d_1} \frac{1}{Z},$$

and thus the channel open probability is

$$P_o = \left(\frac{d_2 d_6 [IP_3] [Ca^{2+}]}{(d_1 d_2 + d_2 [IP_3] + d_3 [Ca^{2+}] + [IP_3] [Ca^{2+}]) (d_5 d_6 + d_7 [\text{Bcl-2}] + d_6 [Ca^{2+}] + [Ca^{2+}] [\text{Bcl-2}])} \right)^3.$$

Here, d_i is the dissociation constant for each binding site. And according to the detailed balance principle, $d_7 = d_5 d_6/d_8$. Consequently, P_o is a function of [IP_3], [Ca^{2+}], and [Bcl-2]. From Fig. 5(a) we can see that with fixed [IP_3] and [Ca^{2+}], P_o presents a progressive decreasing trend with increasing [Bcl-2].

In the indirect mechanism, Bcl-2 regulates the conversion of pDARPP-32 to DARPP-32, which indirectly controls the ratio between IP_3R and pIP_3R, and thereby the maximal Ca^{2+} channel flux. Considering that system (16) is in steady state for [Ca^{2+}] = 0.2 μM, we obtain the expression of [pDARPP-32] by solving the equation $v_3 - v_4 = 0$, and then insert it into v_2. Then we derive the expression of IP_3R by solving $v_1 - v_2 = 0$. By substituting IP_3R into formula (6), we can give the expression of the maximal Ca^{2+}channel flux with respect to [Bcl-2] ([Bcl-2] is denoted as B for convenience),

$$u_1 = -\frac{0.014(5.7\times10^{24}B^8 - 3.85\times10^{17}\alpha B^4 - 3.03\times10^{21}B^4 + 8.86\times10^{13}\alpha + 4.33\times10^{17} - \beta)}{3.42\times10^{23}B^8 - 4.27\times10^{16}\alpha B^4 - 1.57\times10^{20}B^4 + 9.84\times10^{12}\alpha + 2.05\times10^{16}} + 0.17,$$

where

$$\alpha = 10^3 \times \sqrt{3.04\times10^8 B^8 - 1.92\times10^5 B^4 + 32.1},$$
$$\beta = 10^{15} \times \sqrt{\beta_4 - \beta_3 + \beta_2 - \beta_1 + \beta_0},$$

with

$$\beta_4 = 7.06\times10^{19}B^{16},$$
$$\beta_3 = \left(3.52\alpha + 7.63\times10^4\right)\times10^{12}B^{12},$$
$$\beta_2 = \left(2.61\alpha + 3.13\times10^4\right)\times10^{9}B^{8},$$
$$\beta_1 = \left(6.66\alpha + 5.76\times10^4\right)\times10^{5}B^{4},$$
$$\beta_0 = 57.9\alpha + 4\times10^5.$$

As shown in Fig. 5(b), u_1 shows an ultrasensitive response to [Bcl-2], i.e., small increases in the level of Bcl-2 lead to large decreases in the maximal Ca^{2+} channel flux within the physiological range of Bcl-2 (0.05 μM to 0.65 μM,[34] highlighted in green).

One may think that the sharp relationship between the maximal Ca^{2+} channel flux and [Bcl-2] is ascribed to that the Hill coefficient in Eq. (13), which reflects the regulation strength of Bcl-2 on the conversion of pDARPP-32 into DARPP-32, is equal to 4. In fact, the lower Hill coefficient, such as 1, yields the same qualitative result (Fig. S2).

Using mathematical analysis, we confirm the inhibitory effect of Bcl-2 on Ca^{2+} release, and further prove that the indirect mechanism is more efficient than the direct mechanism, especially in the physiological concentration range of Bcl-2.

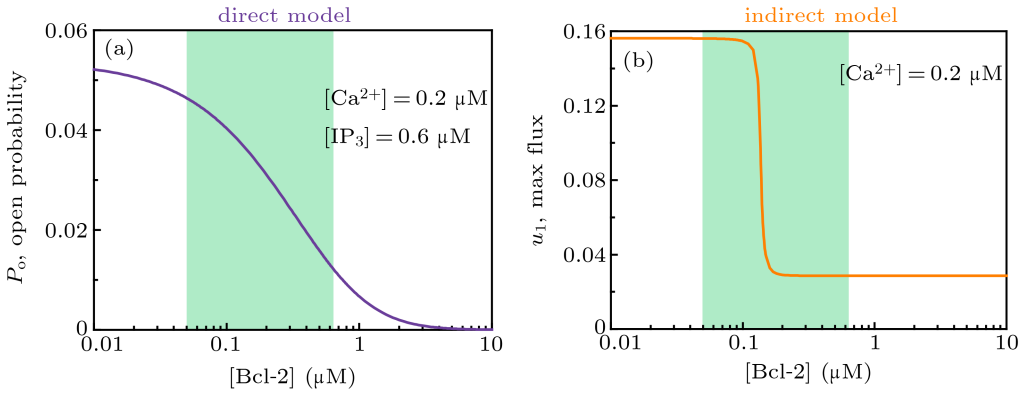

Fig. 5. Mathematical analysis results. (a) For the direct mechanism model, the channel open probability is plotted versus [Bcl-2] when [IP_3] = 0.6 μM and [Ca^{2+}] = 0.2 μM. (b) For the indirect mechanism model, the maximal Ca^{2+} channel flux is plotted versus [Bcl-2] when [Ca^{2+}] = 0.2 μM. The physiological range of Bcl-2 is highlighted in green.

3.5. Dual-mechanism model analysis

Given the different efficiency of the direct and indirect mechanisms on Ca^{2+} release, we lastly examine their combination effect on Ca^{2+} signal. For a fixed amount of Bcl-2, it is unclear how many Bcl-2 are involved in the direct or indirect mechanism. As mentioned above, we use β $(1-\beta)$ to represent the percentage of Bcl-2 involved in the direct (indirect) mechanism

Figure 6 shows the one-parameter bifurcation diagrams of [Ca^{2+}] against [Bcl-2] for different combinations of the direct and indirect mechanisms. Compared with Fig. 3, we can see that when $\beta = 0.5$, the one-parameter bifurcation diagram looks like a hybrid of the direct and indirect mechanisms (Fig. 6(b)); when $\beta = 0.8$, it looks more like the one of the direct mechanism (Fig. 6(a)); when $\beta = 0.2$, it looks more like the one of the indirect mechanism (Fig. 6(c)). In addition, the parameter range of [Bcl-2] that causes Ca^{2+} oscillations in the dual-mechanism model seems to be wider than the one in either single mechanism.

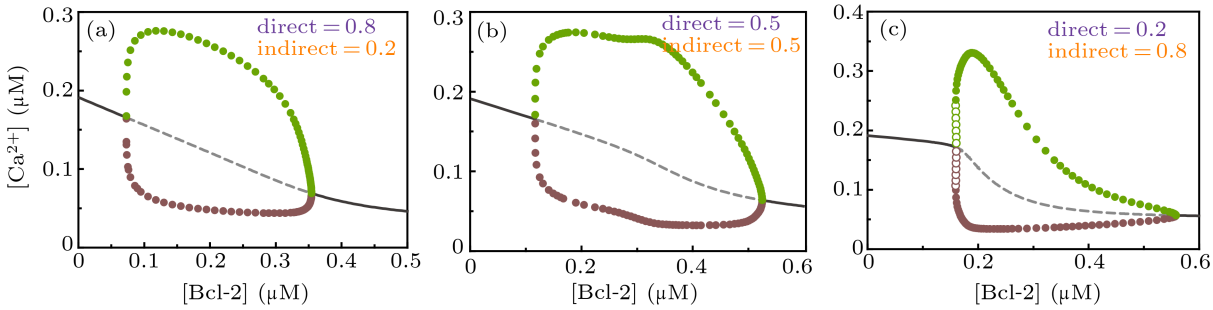

Fig. 6. One-parameter bifurcation diagrams of $[Ca^{2+}]$ against [Bcl-2] for dual-mechanism model under different combination of direct and indirect mechanisms, i.e., $\beta = 0.8$ (a), $\beta = 0.5$ (b), and $\beta = 0.2$ (c). The graphical notations are similar to those in Fig. 3.

Generally, when two factors act together, their combination effect can be classified into three main types: additive, if the combination effect is equal to the sum of the effect of individual factors; synergistic, if the combination effect is higher than additive; and antagonistic, if the combination effect is lower than additive.[35]

As the dual-mechanism expands the range of Bcl-2 that triggers Ca^{2+} oscillations, the direct and indirect mechanisms act synergistically.

4. Discussion

As a critical modulator of IP_3R,[36] Bcl-2 prevents Ca^{2+} release from the ER either by directly binding the IP_3R[12] or by indirectly decreasing IP_3R phosphorylation through a negative feedback loop.[16] The apparent complexity of the two mechanisms is further increased by their intertwined relationship with each other. Furthermore, a research connecting these two mechanisms is still lacking. By developing mathematical models for the direct and indirect mechanisms and then combining them into a dual-mechanism model, we provide a holistic view of how Bcl-2 represses Ca^{2+} release from the ER theoretically.

The major findings of the present study are that (1) although Bcl-2 acts differentially in the direct and indirect mechanisms, its inhibitory effect on Ca^{2+} signal is similar in both mechanisms; (2) the indirect mechanism is more potent than the direct mechanism in inhibiting Ca^{2+} signal; and (3) the direct and indirect mechanisms suppress Ca^{2+} signal in a synergistic manner, which may expand the richness in the message conveyed by Bcl-2.

Since it is still challenging to determine how much the inhibitory effect of Bcl-2 on Ca^{2+} signal results from purely the direct mechanism and how much from the indirect mechanism, the second and third findings ought to be assessed *in vivo* and the full complexity of the relationship between the two mechanisms ought to be further characterized in more detail. Nevertheless, our work can be viewed as a starting point to uncover their complex relationship.

An appropriate elevation of Ca^{2+} is critical for cell survival, while high amplitude Ca^{2+} elevation triggers cell death including apoptosis. Bcl-2, directly or indirectly, regulates IP_3R, thereby dampening its proapoptotic Ca^{2+}-release properties and promoting the survival of cancer cells.[37,38] This may allow for exquisite control of Bcl-2's inhibitory property on Ca^{2+} signal and thus be important for cancer treatment by modulating the direct and indirect mechanisms together. Given that some Bcl-2 inhibitors have progressed into clinical studies,[39,40] the two complementing mechanisms need to be quantitatively considered in order to develop precision medicines that target cancers.

Overall, this study provides a theoretical understanding for the direct and indirect mechanisms of Bcl-2 suppression in Ca^{2+} release, which might be important in terms of efforts to target Bcl-2 for cancer treatment to achieve optimal effect. In addition, our findings may be useful to understand how other members of the Bcl-2 protein family, including Bcl-xL[41] and BOK,[42] modulate Ca^{2+} release from the ER.

References

[1] Berridge M J, Bootman M D and Roderick H L 2003 *Nat. Rev. Mol. Cell Biol.* **4** 517
[2] Orrenius S, Zhivotovsky B and Nicotera P 2003 *Nat. Rev. Mol. Cell Biol.* **4** 552
[3] Qi H, Li X, Jin Z, Simmen T and Shuai J 2020 *iScience* **23** 101671
[4] Chong S J F, Marchi S, Petroni G, Kroemer G, Galluzzi L and Pervaiz S 2020 *Trends Cell Biol.* **30** 537
[5] Distelhorst C W 2018 *BBA-Mol. Cell Res.* **1865** 1795
[6] Bezprozvanny I, Watras J and Ehrlich B E 1991 *Nature* **351** 751
[7] Alzayady K J, Wang L, Chandrasekhar R, Wagner L E, Van Petegem F and Yule D I 2016 *Sci. Signal.* **9** ra35
[8] Boehning D, Patterson R L, Sedaghat L, Glebova N O, Kurosaki T and Snyder S H 2003 *Nat. Cell Biol.* **5** 1051
[9] Yin Z, Qi H, Liu L and Jin Z 2017 *BioSystems* **162** 44
[10] Bonneau B, Prudent J, Popgeorgiev N and Gillet G 2013 *BBA-Mol. Cell Res.* **1833** 1755
[11] Parys J B 2014 *Sci. Signal.* **7** pe4
[12] Rong Y, Bultynck G, Aromolaran A S, Zhong F, Parys J B, De Smedt H, Mignery G A, Roderick H L, Bootman M D and Distelhorst C W 2009 *Proc. Natl. Acad. Sci. USA* **106** 14397
[13] Monaco G, Decrock E, Akl H, Ponsaerts R, Vervliet T, Luyten T, De Maeyer M, Missiaen L, Distelhorst C and De Smedt H 2012 *Cell Death Differ.* **19** 295
[14] Ivanova H, Luyten T, Decrock E, Vervliet T, Leybaert L, Parys J B and Bultynck G 2017 *Cell Calcium* **62** 41
[15] Monaco G, La Rovere R, Karamanou S, Welkenhuyzen K, Ivanova H, Vandermarliere E, Di Martile M, Del Bufalo D, De Smedt H, Parys J B, Economou A and Bultynck G 2018 *FEBS J.* **285** 127
[16] Chang M, Zhong F, Lavik A R, Parys J B, Berridge M J and Distelhorst C W 2014 *Proc. Natl. Acad. Sci. USA* **111** 1186

[17] Li X, Zhong J, Gao X, Wu Y, Shuai J and Qi H 2017 *Chin. Phys. B* **26** 128703
[18] Qi H, Jiang Y, Yin Z, Jiang K, Li L and Shuai J 2018 *Phys. Chem. Chem. Phys.* **20** 1964
[19] Qi H, Xu G, Peng X, Li X, Shuai J and Xu R 2020 *Phys. Rev. E* **102** 062422
[20] Li X, Zhong C, Wu R, Xu X, Yang Z, Cai S, Wu X, Chen X, Yin Z, He Q, Li D, Xu F, Yan Y, Qi H, Xie C, Shuai J and Han J 2021 *Protein & Cell* **2021** 1
[21] Niu S, Shuai J and Qi H 2017 *Acta Phys. Sin.* **66** 238701 (in Chinese)
[22] De Young G W and Keizer J 1992 *Proc. Natl. Acad. Sci. USA* **89** 9895
[23] Wagner L E, Li W and Yule D I 2003 *J. Biol. Chem.* **278** 45811
[24] Tang T, Tu H, Wang Z and Bezprozvanny I 2003 *J. Neurosci.* **23** 403
[25] Ferrell J E and Ha S H 2014 *Trends Biochem. Sci.* **39** 496
[26] Li H, Rao A and Hogan P G 2011 *Trends Cell Biol.* **21** 91
[27] Parys J and Bezprozvanny I 1995 *Cell Calcium* **18** 353
[28] Svenningsson P, Nishi A, Fisone G, Girault J A, Nairn A C and Greengard P 2004 *Annu. Rev. Pharmacol. Toxicol.* **44** 269
[29] Shin S Y, Choo S M, Kim D, Baek S J, Wolkenhauer O and Cho K H 2006 *FEBS Lett.* **580** 5965
[30] Neves S R, Tsokas P, Sarkar A, Grace E A, Rangamani P, Taubenfeld S M, Alberini C M, Schaff J C, Blitzer R D and Moraru I I and Iyengar R 2008 *Cell* **133** 666
[31] Tyson J J, Chen K C and Novak B 2003 *Curr. Opin. Cell Biol.* **15** 221
[32] Shuai J, Yang D, Pearson J and Rüdiger S 2009 *Chaos* **19** 037105
[33] Cai X, Li X, Qi H, Wei F, Chen J and Shuai J 2016 *Phys. Biol.* **13** 056005
[34] Lindner A U, Prehn J H M and Huber H J 2013 *Mol. Biosyst.* **9** 2359
[35] Liu Y and Zhao H 2016 *Bioinformatics* **32** 3782
[36] Ivanova H, Vervliet T, Monaco G, Terry L E, Rosa N, Baker M R, Parys J B, Serysheva I I, Yule D I and Bultynck G 2019 *CSH Perspect. Biol.* **12** a035089
[37] Greenberg E F, Lavik A R and Distelhorst C W 2014 *BBA-Mol. Cell Res.* **1843** 2205
[38] Monteith G R, Prevarskaya N and Roberts-Thomson S J 2017 *Nat. Rev. Cancer* **17** 373
[39] Vervloessem T, Kerkhofs M, La Rovere R M, Sneyers F, Parys J B and Bultynck G 2018 *Cell Calcium* **70** 102
[40] Singh R, Letai A and Sarosiek K 2019 *Nat. Rev. Mol. Cell Biol.* **20** 175
[41] Yang J, Vais H, Gu W and Foskett J K 2016 *Proc. Natl. Acad. Sci. USA* **113** E1953
[42] Carpio M A, Means R E, Brill A L, Sainz A, Ehrlich B E and Katz S G 2021 *Cell Rep.* **34** 108827